Electron Exchange Reactions and Redox and Magnetic Properties of the Cobalt(III) and Cobalt(II) Complexes of the Encapsulating Ligand 3,13-Dithia-6,10,16,19-tetraazabicyclo[6.6.6]icosane (N_4S_2sar). Crystal Structure of the Cobalt(II) Complex $[Co(HN_4S_2sar)](ClO_4)_2$

Therese M. Donlevy,[1a] Lawrence R. Gahan,*[1a] and Trevor W. Hambley[1b]

Department of Chemsitry, The University of Queensland, Brisbane, QLD 4072, Australia, and School of Chemistry, The University of Sydney, Sydney, NSW 2006, Australia

Received October 21, 1993®

The redox, magnetic, structural, and electron transfer properties of the cobalt(III) and cobalt(II) complexes of an encapsulating ligand based on 3,13-dithia-6,10,16,19-tetraazabicyclo[6.6.6]icosane (N_4S_2sar) have been investigated. The cobalt(II) complex $[Co(HN_4S_2sar)]^{2+}$ crystallizes in the orthorhombic crystal system, space group *Pmcn* with $a = 8.804(2)$ Å, $b = 12.554(2)$ Å, $c = 21.021(8)$ Å, and $Z = 4$. The structure was refined to $R = 0.050$. The average Co–N bond length is 2.102(7) Å, and a marked elongation in one Co–S bond (2.495(2) Å) in comparison with the other (2.288(2) Å) is apparent. The solution magnetic moment of the Co(II) complex $[Co(AMN_4S_2sarH)]^{3+}$ was found to be 2.88 μ_B, a value inconsistent with either a high- or low-spin condition for this species. The Co(III)/Co(II) reduction potentials for the range of N_4S_2sar complexes were established using cyclic voltammetric methods. The reduction potentials $E°$ (V vs SHE) ranged from +0.022 V for $[Co(NON_4S_2sar)]^{3+/2+}$ to −0.156 V for $[Co(HN_4S_2sar)]^{3+/2+}$. The Marcus cross correlation was used to calculate the self-exchange rates (k_{11}) of the N_4S_2sar complexes from the bimolecular rate information obtained after cross reactions between the cobalt(III) complexes $[Co(XN_4S_2sar)]^{n+}$ with the cobalt(II) complex $[Co(AMMEN_6sarH)]^{3+}$ (X = AM, $k_{11} = 0.72(0.20) \times 10^3$ M^{-1} s^{-1}; X = CL, $k_{11} = 0.84(0.20) \times 10^3$ M^{-1} s^{-1}; X = H, $k_{11} = 1.84(0.30) \times 10^3$ M^{-1} s^{-1}; X = AZA, $k_{11} = 1.12(0.22) \times 10^3$ M^{-1} s^{-1}) or with $[Co(diCLN_6sar)]^{2+}$ (X = CL, $k_{11} = 1.71(0.16) \times 10^3$ M^{-1} s^{-1}). The self exchange rate for $[Co(AMMEN_6sarH)]^{4+/3+}$ was determined by polarimetric methods to be 0.15 M^{-1} s^{-1}. The self exchange electron transfer rates for $[Co(AMN_4S_2sarH)]^{4+/3+}$ and $[Co(HN_4S_2sar)]^{3+/2+}$ were determined directly, using NMR methods, as $1.70(0.5) \times 10^3$ M^{-1} s^{-1} and $1.22(0.16) \times 10^4$ M^{-1} s^{-1}, respectively. The contributions of the inner-sphere reorganization energies for these N_4S_2sar complexes have been investigated.

Introduction

Encapsulated complexes based on 3,6,10,13,16,19-hexaazabicyclo[6.6.6]icosane (sar) have been shown to offer intriguing prospects for studies of the spectroscopic, electrochemical, and structural aspects of the metal ions enclosed within the three-dimensional cavity defined by the ligand.[1-14] Of special interest have been electron transfer studies involving these encapsulated complexes, reactions for which the complexes are particularly suited because of the outer-sphere nature of the reaction.[15-24] For the cobalt(III/II) hexaamine complexes (N_6sar), the self-exchange rates for electron transfer have generally been found to be on the order of 5 M^{-1} s^{-1}.[15] The rate of electron transfer for the 3,6,10,13,16,19-hexathiabicyclo[6.6.6]icosane complex, $[Co(Me_2S_6sar)]^{3+/2+}$, was found to be of the order of 10^4 M^{-1} s^{-1},[23] similar to that reported for the cobalt complexes of 3,13,-16-trithia-6,10,19-triazabicyclo[6.6.6]icosane (N_3S_3sar).[16,23] Analysis of the electron transfer reactions have been undertaken within the framework of the Marcus theories for outer-sphere electron transfer,[25,26] and, within the limits of the theories, correlations between the observed and calculated rates of electron transfer have been remarkably good.[15] The enhancement in rate for the N_3S_3sar and S_6sar complexes over the N_6sar systems has been ascribed in large part to the low-spin condition of the reactants, both cobalt(III) and cobalt(II), and the corresponding reduction in internal reorganization energy.[16,23,27]

The recent report[11] of the preparation of encapsulated

* Author to whom correspondence should be sent.
® Abstract published in *Advance ACS Abstracts,* May 1, 1994.

(1) (a) The University of Queensland. (b) The University of Sydney.
(2) Creaser, I. I.; Harrowfield, J. M.; Herlt, A. J.; Sargeson, A. M.; Springborg, J.; Geue, R. J.; Snow, M. R. *J. Am. Chem. Soc.* **1977**, *99*, 3181.
(3) Creaser, I. I.; Geue, R. J.; Harrowfield, J. M.; Herlt, A. J.; Snow, M. R.; Springborg, J. *J. Am. Chem. Soc.* **1982**, *104*, 6016.
(4) Geue, R. J.; Hambley, T. W.; Harrowfield, J. M.; Sargeson, A. M.; Snow, M. R. *J. Am. Chem. Soc.* **1984**, *106*, 5478.
(5) Sargeson, A. M. *Pure Appl. Chem.* **1984**, *56*, 1603.
(6) Sargeson, A. M. *Chem. Br.* **1979**, *15*, 23.
(7) Sargeson, A. M. *Pure Appl. Chem.* **1986**, *58*, 1511.
(8) Bond, A. M.; Lawrance, G. A.; Lay, P. A.; Sargeson, A. M. *Inorg. Chem.* **1983**, *22*, 2010.
(9) Martin, L. L.; Martin, R. L.; Murray, K. S.; Sargeson, A. M. *Inorg. Chem.* **1990**, *29*, 1387.
(10) Gahan, L. R.; Hambley, T. W.; Sargeson, A. M.; Snow, M. R. *Inorg. Chem.* **1982**, *21*, 2699.
(11) Donlevy, T. M.; Gahan, L. R.; Hambley, T. W.; Stranger, R. *Inorg. Chem.* **1992**, *31*, 4376.
(12) Comba, P. *Inorg. Chem.* **1989**, *28*, 426.
(13) Comba, P.; Sargeson, A. M.; Engelhardt, L. M.; Harrowfield, J. M.; White, A. H.; Horn, E.; Snow, M. R. *Inorg. Chem.* **1985**, *24*, 2325.
(14) Hupp, J. T.; Liu, H. Y.; Lay, P. A.; Petri, W. H. F.; Sargeson, A. M.; Weaver, M. J. *J. Electroanal. Chem.* **1984**, *163*, 371.
(15) Creaser, I. I.; Sargeson, A. M.; Zanella, A. W. *Inorg. Chem.* **1983**, *22*, 4022.
(16) Dubs, R. V.; Gahan, L. R.; Sargeson, A. M. *Inorg. Chem.* **1983**, *22*, 2523.
(17) Bernhard, P.; Sargeson, A. M. *Inorg. Chem.* **1987**, *26*, 4122.
(18) Bakac, A.; Espenson, J. H.; Creaser, I. I.; Sargeson, A. M. *J. Am. Chem. Soc.* **1983**, *105*, 7624.
(19) Balahura, R. J.; Johnson, M. D. *Inorg. Chem.* **1987**, *26*, 3860.
(20) Geue, R. J.; McCarthy, M. G.: Sargeson, A. M. *J. Am. Chem. Soc.* **1984**, *106*, 8282.
(21) Bernhard, P.; Bürgi, H.-B.; Raselli, A.; Sargeson, A. M. *Inorg. Chem.* **1989**, *28*, 3234.
(22) Bernhard, P.; Bull, D. J.; Robinson, W. T.; Sargeson, A. M. *Aust. J. Chem.* **1992**, *45*, 1241.
(23) Osvath, P.; Sargeson, A. M.; Skelton, B. W.; White, A. H. *J. Chem. Soc., Chem. Commun.* **1991**, 1036.
(24) Clark, I. J.; Creaser, I. I.; Engelhardt, L. M.; Harrowfield, J. M.; Krausz, E. R.; Moran, G. M.; Sargeson, A. M.; White, A. H. *Aust. J. Chem.* **1993**, *46*, 111.
(25) Marcus, R. A. *Discuss. Faraday Soc.* **1960**, *29*, 21.
(26) Marcus, R. A. *Annu. Rev. Phys. Chem.* **1964**, *15*, 155.

0020-1669/94/1333-2668$04.50/0

Chart 1

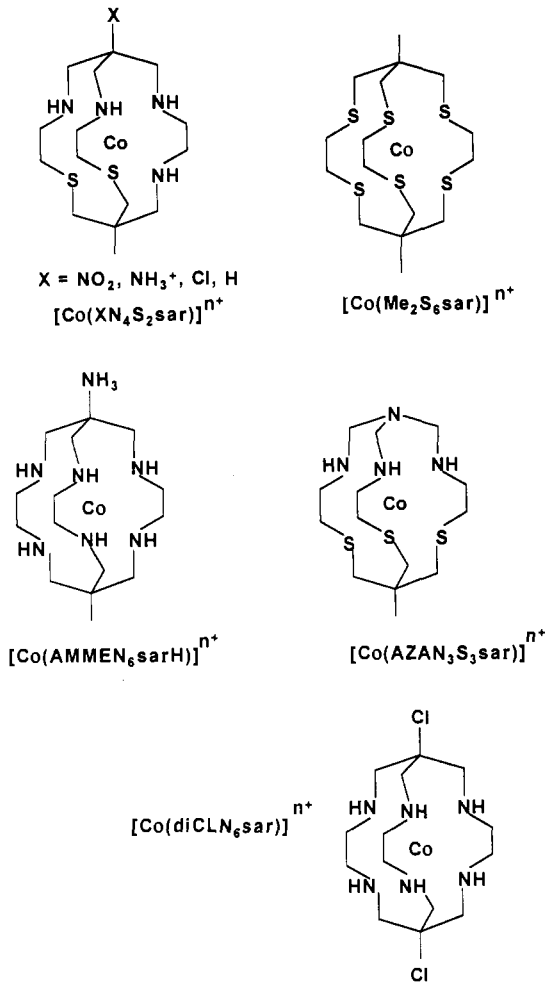

complexes of cobalt(III) based on the 3,13-dithia-6,10,16,19-tetraazabicyclo[6.6.6]icosane (N_4S_2sar) ligand presents the opportunity to further develop studies of electron transfer reactions of encapsulated complexes, particularly the effects of reorganization energies. This paper reports studies of the electron transfer reactions of encapsulated complexes of cobalt(III/II) with this ligand, using the Marcus correlation and direct determination of the rate of self exchange employing T_2 measurements, as well as the single-crystal X-ray structure of a cobalt(II) complex of the proton-capped complex $[Co(HN_4S_2sar)](ClO_4)_2$. The influence and contribution of reorganization energies of the encapsulated complexes are investigated in terms of a semiclassical model of electron transfer reactions.[28-31] For a description of the complexes detailed in this work see Chart 1.

Experimental Section

The complexes $[Co(AZAN_3S_3sar)](ClO_4)_3$,[10] $[Co(AMN_4S_2sarH)]Cl_4$,[11] $[Co(CLN_4S_2sar)](ClO_4)_3$,[11] $[Co(HN_4S_2sar)](ClO_4)_3$,[11] $[Co(AZAN_4S_2sar)](ClO_4)_3$,[11] $[Co(diCLN_6sar)]Cl_3$,[4] and $[Co(AMMEN_6sarH)]Cl_4$[4] were prepared as described previously.

$[Co(HN_4S_2sar)](ClO_4)_2$. $[Co(HN_4S_2sar)](ClO_4)_3$ (0.5 g) was dissolved in water (1 mL) and reduced over zinc amalgam under an atmosphere of nitrogen. The reduced solution was transferred by cannula to a degassed flask containing $NaClO_4$. The dark purple crystals which formed in the solution after allowing it to stand for 12 h were collected and stored under an atmosphere of nitrogen. The crystals were suitable for X-ray structural analysis.

Table 1. Crystal Data for $[Co(HN_4S_2sar)](ClO_4)_2$

crystal system	orthorhombic
space group	*Pmcn*
a, Å	8.804(2)
b, Å	12.554(2)
c, Å	21.021(8)
V, Å^3	2323(1)
d_{calcd}, g cm^{-3}	1.677
formula	$C_{15}H_{32}Cl_2CoN_4O_8S_2$
fw	590.4
Z	4
μ(Mo Kα), cm^{-1}	11.48
λ, Å	0.710 69
T, °C	21
transm coeff	0.470–0.589
R^a	0.050
$R_w{}^a$	0.072
g, k	2.43, 9.2×10^{-4}

$^a R = (\Sigma\|\|F_o| - |F_c\|\|)/\Sigma|F_o|$. $R_w = (\Sigma w^{1/2}\|\|F_o| - |F_c\|\|)/\Sigma w^{1/2}|F_o|$; [$w = g/(\sigma^2 F_o + kF_o^2)$].

X-ray Crystallography. Cell constants were determined by least-squares fits to the setting parameters of 25 independent reflections, measured and refined on an Enraf-Nonius CAD4-F diffractometer with a graphite monochromator. The crystallographic data are summarized in Table 1. Data were reduced, and Lorentz, polarization, and absorption corrections were applied using the Enraf-Nonius structure determination package (SPD).[32] The structure was solved by direct methods using SHELXS-86[33] and was refined by full-matrix least-squares analysis with SHELX-76.[34] The complex was found to lie on and be disordered about a mirror plane. Some atoms were common to each contributor to the disorder. One perchlorate anion was also found to be rotationally disordered over two sites with complimentary occupanices for O(1)–O(4) and O(1′)–O(4′) of 0.76:0.24. Hydrogen atoms were refined or included at calculated sites (C–H, N–H 0.97 Å) with individual isotropic thermal parameters. All other atoms except minor contributors to the disordered perchlorate were refined anisotropically. Scattering factors and anomalous dispersion corrections for Co were taken from ref 35, and for all others the values supplied in SHELX-76 were used. Non-hydrogen atom coordinates are listed in Table 2. The atomic nomenclature is defined in Figure 2.[36] Listings of H atom coordinates, anisotropic thermal parameters, close intermolecular contacts, torsion angles and observed and calculated structure factor amplitudes have been deposited as supplementary material.

Magnetic Susceptibility. Solution magnetic moments were determined by the Evans method.[37] A solution of the cobalt(III) complex (0.1 g, dissolved in 2 mL of H_2O) was reduced to cobalt(II) as described above and added under a stream of nitrogen to a 5-mm PP-528 Wilmad NMR tube. A sealed capillary containing H_2O was inserted and kept axially orientated by the Teflon plug through which the capillary passed. Measurements were performed on both a Varian EM360 spectrometer and a Bruker AC-200F spectrometer. Suitable bulk susceptibility corrections were made for measurements performed on the superconducting magnet.[38-40]

Cobalt(II) NMR Spectra. The Co(III) complex was reduced to Co(II) as described above. Concentrated solutions were prepared, typically 0.3 g of complex dissolved in 3 mL of D_2O. The oxygen-sensitive solutions

(27) Hambley, T. W.; Snow, M. R. *Inorg. Chem.* **1986**, *25*, 1378.
(28) Brunschwig, B. S.; Logan, J.; Newton, M. D.; Sutin, N. *J. Am. Chem. Soc.* **1980**, *102*, 5798.
(29) Sutin, N. *Acc. Chem. Res.* **1982**, *15*, 275.
(30) Sutin, N. *Prog. Inorg. Chem.* **1983**, *30*, 441.
(31) Brunschwig, B. S.; Creutz, C.; Macartney, D. H.; Sham, T. K.; Sutin, N. *Faraday Discuss. Chem. Soc.* **1982**, *74*, 113.
(32) Enraf-Nonius Structure Determination Package. Enraf-Nonius, Delft, Holland, 1985.
(33) Sheldrick, G. M. SHELXS-86. In *Crystallographic Computing 3*; Sheldrick, G. M., Kruger, C., Goddard, R., Eds.; Oxford University Press: Oxford, U.K., 1985; pp 175–189.
(34) Sheldrick, G. M. SHELXS-76. A Program for X-Ray Crystal Structure Determination. University of Cambridge, England, 1976.
(35) Cromer, D. T.; Waber, J. T. *International Tables for X-Ray Crystallography*; Kynoch Press: Birmingham, England, 1974; Vol. IV.
(36) Figures were drawn with ORTEP (Johnson, C. K. *ORTEP, A Thermal Ellipsoid Plotting Program*; Oak Ridge National Labs: Oak Ridge, TN, 1965).
(37) Evans, D. F. *J. Chem. Soc.* **1959**, 2003.
(38) Live, D. H.; Chan, S. I. *Anal. Chem.* **1970**, *42*, 791.
(39) Becconsall, J. K.; Daves, G. D., Jr.; Anderson, W. R., Jr. *J. Am. Chem. Soc.* **1970**, *92*, 430.
(40) Becker, E. D. *High Resolution NMR: Theory and Chemical Applications*; Academic Press; New York, 1980; Chapter 3, pp 42–61.

Table 2. Positional Parameters ($\times 10^4$) for $[Co(HN_4S_2sar)](ClO_4)_2$

	x	y	z
Co(1)	2500	1963(1)	1278(1)
S(1)	4644(2)	2607(2)	798(1)
S(2)	1443(3)	1345(2)	241(1)
N(1)	1367(7)	3414(5)	1115(3)
N(2)	3657(8)	2328(6)	2153(3)
N(3)	1906(8)	404(5)	1389(3)
N(4)	510(8)	1652(6)	1809(5)
C(1)	2500	4249(7)	-586(4)
C(2)	2500	3457(4)	-25(3)
C(3)	3924(6)	3699(4)	350(3)
C(4)	2500	2348(7)	-306(4)
C(5)	5195(8)	3384(6)	1465(3)
C(6)	2500	280(6)	225(4)
C(7)	5270(8)	2698(6)	1998(4)
C(8)	2500	-306(5)	841(4)
C(9)	3911(13)	1338(8)	2555(4)
C(10)	2500	-91(6)	1995(3)
C(11)	2500	690(6)	2530(3)
Cl(1)	2500	-3438(1)	1128(1)
O(1)	2500	-2711(15)	1571(10)
O(2)	1560(17)	-4313(9)	1267(5)
O(3)	2500	-3201(13)	470(5)
O(1′)	1143(26)	-2791(19)	1180(11)
O(2′)	2500	-2666(31)	1714(19)
O(3′)	3368(48)	-2991(30)	659(20)
O(4′)	4019(26)	-3633(28)	1163(10)
Cl(2)	2500	4610(1)	3293(1)
O(5)	2500	4769(10)	2645(3)
O(6)	3802(10)	4424(11)	3598(6)
O(7)	1821(14)	5504(10)	3557(7)
O(8)	1517(18)	3723(11)	3358(7)

were kept in a nitrogen atmosphere during transfer to the 10-mm NMR tubes. A vortex plug was inserted to minimize the surface area susceptible to oxidation. The cap of the NMR tube was sealed with Parafilm. A pulsewidth of 14 μs (90°) with a pulse delay of 2 ms was employed for the ^1H and ^{13}C NMR experiments (10 mm probe, Bruker AC-200F MHz NMR spectrometer). Both ^{13}C and ^1H NMR spectra were collected using the automated sequence, NOROLDEC.AU, to minimize base-line roll. All spectra were initially run upon the maximum spectral width (1 000 000 Hz) to obtain optimum frequency width and positional parameters, excluding the possibility of folding. Pertinent parameters are as follows: ^{13}C, O1 = -12 000, SW = 41 666.667 Hz, SI = 8192, DP = 12H CPD; ^1H, O1 = 10 000, SW = 41 666.667 Hz, SI = 16384, DP = 10L PO, RD = 0.2 s. Selective decoupling experiments and the 135° DEPT sequence promoted identification of the methyl peak from the complex in both the ^1H and ^{13}C spectra.

$[Co(HN_4S_2sar)]^{2+}$. ^{13}C NMR (D_2O, dioxane = 0 ppm): δ 81.4, -72.1 (CH_3), -120.8, -153.3, -163.2, -216.3, -234.6, -260.6, -284.0, -333.8, -345.0 ppm. ^1H NMR (D_2O, NaTPS): δ 144.4, 107.6, 98.9, 89.1, 80.7, 66.5, 62.6, 55.2, 51.2, 49.0, 42.9, 40.2, 31.5, 29.7, 13.4 (CH_3), 6.9, -1.1, -6.3, -10.0, -14.8, -15.8 ppm.

$[Co(AMN_4S_2sarH)]^{3+}$. ^{13}C NMR (D_2O, dioxane = 0 ppm): δ 90.2, -2.2, -71.0 (CH_3), -130.4, -154.4, -165.7, -177.5, -187.6, -197.7, -219.3, -230.6, -282.4, -336.3, -343.2 ppm. ^1H NMR (D_2O, NaTPS): δ 128.0, 117.6, 99.9, 97.5, 72.2, 67.1, 64.4, 61.8, 59.8, 54.4, 52.5, 49.3, 47.9, 43.1, 34.2, 24.6, 23.7, 22.7, 16.1 (CH_3), 14.6, -6.3, -9.1, -13.2, -18.7, -22.0 ppm.

Electrochemical Measurements. Cyclic voltammograms were recorded with a BAS-100 electrochemical device with a standard three-electrode system. The working electrode was either glassy carbon or gold, with a platinum auxiliary. The reference electrode was Ag/AgCl (saturated $NaClO_4$, +231 mV vs SHE). The salt bridge was filled with the electrolyte solution (0.1 M $NaClO_4$ or 0.1 M $HClO_4$) employed in the working compartment. The electrode surfaces were cleaned with alumina prior to, and between, measurements. Measurements were recorded at 25 °C after the solutions had been degassed with nitrogen. Each reduction potential was recorded at a number of scan rates, ranging from 5 to 500 mV s^{-1}.

Kinetic Measurements. (i) Polarimetry. The rate of self exchange electron transfer for $[Co(AMMEN_6sarH)]^{4+/3+}$ was measured with a Perkin-Elmer P22 spectropolarimeter, using a previously described procedure.[3] The wavelength employed was 520 nm. Solutions were prepared in 0.1 M $NaClO_4$/0.1 M $HClO_4$ and the concentrations of reactants determined by UV–vis spectroscopy prior to use.

(ii) Cross Reactions. Solutions of the cobalt complexes of XN_4S_2sar (X = AM, CL, H, AZA) were prepared in 0.1 M $NaClO_4$/0.1 M $HClO_4$ and the concentrations of reactants determined by UV–vis spectroscopy prior to use. The electron transfer cross reaction rates were monitored using a Gibbs Durrum D-110 stopped flow reactor equipped with a D-131 photometric log amplifier and a Biomation 805 wave-form recorder. The Co(II) complex was prepared by reduction over zinc amalgam and all solutions were degassed using argon. The transfer syringes and the work station (stopped-flow reactor) were placed in a continuously flushed nitrogen atmosphere. The syringes and flowlines were flushed first with Tris buffer solutions (5×10^{-2} M, pH = 8) followed by a buffer solution of sodium dithionite (5×10^{-3} M) and were left overnight to ensure the dithionite would scavenge any adsorbed O_2(g). Prior to use, the apparatus was placed in a nitrogen glovebag, and the flowlines and syringes were flushed of the dithionite solution with degassed buffer. The syringes were each flushed with 10 mL of degassed Millipore water, followed by two volumes of reactant before measurements were recorded. To minimize oxidation, the transfer syringes containing the O_2-sensitive Co(II) species also contained a piece of amalgamated zinc. All measurements were carried out at 25 ± 0.1 °C. A tungsten halide lamp was utilized for the measurements. The wavelengths used were as follows: $[Co(AMMEN_6sarH)]^{3+}$, λ = 390, 490, 500, 510 nm; reactions with $[Co(diCLN_6sar)]^{2+}$, λ = 390, 490 nm. Absorbance versus time data were collected at each wavelength (an average of 10 observations per wavelength for a given ratio of reactants). All reactions were carried out under pseudo-first-order conditions where the concentration of the Co(II) species was at least 10 times greater than that of the Co(III). The decay data was fitted to the single exponential function $a^* \exp(-b^*x) + c$, where a is the total change in absorbance, b is the first-order rate constant, k_{obs}, and c is the x-intercept ($c = 0$ for an ideal exponential decay). Plots were generally linear for at least 4 half-lives.

(iii) NMR Line Broadening. Chloride salts of the $[Co(HN_4S_2sar)]^{3+}$ and $[Co(AMN_4S_2sarH)]^{4+}$ complexes were hygroscopic and were therefore kept in a vacuum desiccator and weighed into sealable vials under a nitrogen atmosphere. All solutions were prepared immediately prior to the experiment. Optimum concentrations, prior to mixing, of the Co(III) and Co(II) solutions were approximately 1×10^{-1} and 5×10^{-2} M, respectively. The complexes were dissolved in a mixture of acidic D_2O (10 μL HCl in 10 mL) and dioxane (20 drops in 10 mL). Dioxane was employed as an internal standard, initially. The solutions were purged with nitrogen gas for 2 h, and the Co(II) complex was produced by reduction of the corresponding Co(III) complex over amalgamated zinc in a nitrogen atmosphere. The solutions for the NMR experiment were prepared under an atmosphere of nitrogen in a VAC Drylab. Gilson micropipets were employed to deliver aliquots of the Co(II), Co(III), and D_2O solutions. The concentration of the Co(III) solution was kept constant and the concentration of the Co(II) species was varied in such a way that the Co(III)/Co(II) ratio ranged between 10:1 and 50:1 for selected experiments. The total volume was maintained at 0.6 mL, and the tubes were sealed with rubber septa. To minimize oxidation, the samples were maintained in a nitrogen atmosphere prior to the NMR experiment. The half-height line width of the methyl resonance in the ^1H NMR spectrum was monitored for exchange-induced broadening.

(iv) T_2 Experiments. Solutions were prepared as for the NMR line-broadening experiments, except that the dioxane was omitted. ^1H NMR spectra were run using a modified Hahn echo sequence: D1–90–VD–180–VD–FID, where D1, the pre-equilibrium delay, was set to 2 s; VD (τ) ranged from 10 μs to $4T_2$. The 90° pulse widths for the encapsulated complexes were determined without the directional decoupler connected and found to equal 14μs. The decay of signal intensity is described by $I = I_0 \exp(-2\tau/T_2)$.[41-43] An average of 32 measurements were taken per concentration and 16 scans per τ value.

Results and Discussion

The synthesis and characterization of encapsulated complexes of the ligand 3,13-dithia-6,10,16,19-tetraazabicyclo[6.6.6]icosane (N_4S_2sar), have been described previously,[11] as has the nomenclature employed for the encapsulated complexes.[8,11] Throughout

(41) Swift, T. J. In *NMR of Paramagnetic Molecules: Principles and Applications*; La Mar, G. N., Horrocks, W. DeW., Holm, R. H., Eds.; Academic Press: New York/London, 1973. Chapter 2, pp 53–83.
(42) Derome, A. E. *Modern NMR Techniques for Chemistry Research*; Pergamon Press Books Ltd.: London, 1990; Vol. 6 pp 65–100.
(43) Martin, M. L.; Martin, G. J.; Delpuech, J. J. *Practical NMR Spectroscopy*; Heyden & Son Ltd.: London, 1980.

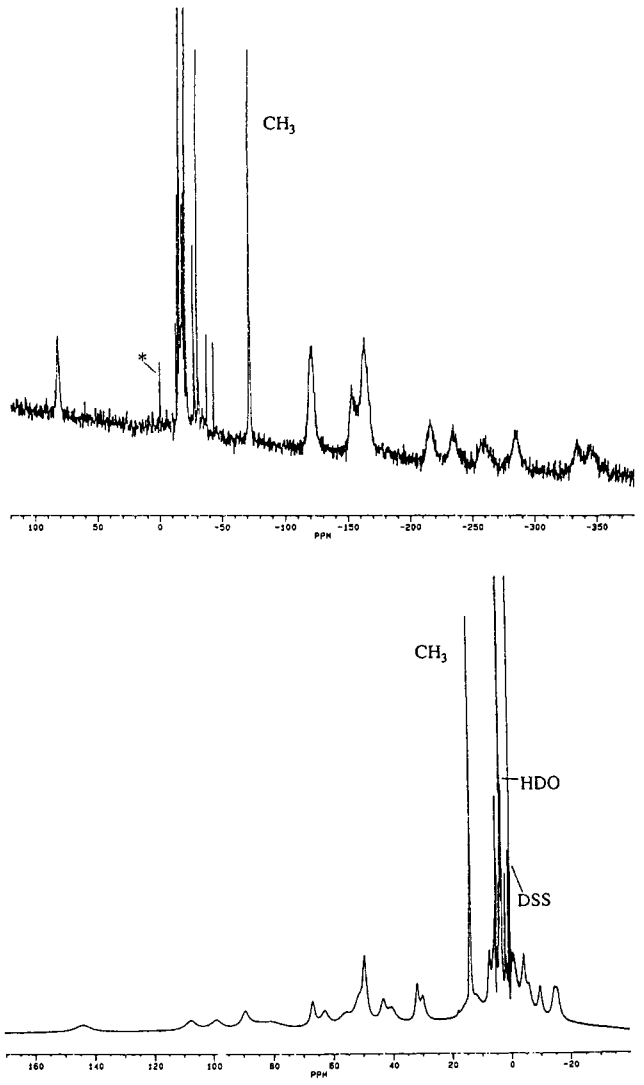

Figure 1. ^1H (bottom) and ^{13}C NMR (top) spectra for $[Co(HN_4S_2sar)]^{2+}$ (* = dioxane).

this work the additional abbreviations for the cobalt(III) complexes $[Co(XN_4S_2sar)]^{n+}$ (X = AM, n = 4; X = NO, CL, H, AZA, n = 3) will be employed.[8] Reduction of the Co(III) complexes under an atmosphere of nitrogen with amalgamated zinc results in the corresponding Co(II) species, although for the NO-capped complex prolonged exposure to reducing conditions results in the AM-capped complex, as noted previously.[15]

^1H and ^{13}C NMR Spectra for $[Co(HN_4S_2sar)]^{2+}$. ^1H and ^{13}C NMR spectra for the Co(II) complex $[Co(HN_4S_2sar)]^{2+}$ are shown in Figure 1. The NMR spectra of Co(II) complexes of encapsulated ligands have not been reported previously. As with ^{13}C NMR spectra of Co(III) complexes, the Co(II) complexes of XN_4S_2sar ligands possess lower symmetry than those with the analogous XN_3S_3sar ligands. No significant differences were observed in the spectra of XN_4S_2sar (X = AM, H) with change in the capping group. In both the ^{13}C and ^1H NMR spectra, one resonance peak was far more intense and shaprer than the other broad resonances. Positive assignment of this sharp resonance in the ^{13}C NMR spectrum of $[Co(AMN_4S_2sarH)]^{3+}$ as being the apical CH_3 group was achieved through application of a 135° DEPT pulse experiment in which the CH_3 was inverted. In the ^1H NMR spectra of these Co(II) complexes a similar intense resonance was observed. ^{13}C off-resonance decoupling experiments, utilising the frequency of this intense ^1H signal confirmed that this resonance was indeed due to the CH_3 group.

Crystal Structure of $[Co(HN_4S_2sar)](ClO_4)_2$. The Co(II) complexes may be isolated as purple, air-sensitive crystals from aqueous $NaClO_4$ solution. The structure of $[Co(HN_4S_2sar)](ClO_4)_2$ consists of the complex cation and two perchlorate anions. The numbering scheme for the complex cation is shown in Figure 2. There are significant disordering effects present in the structure. The atoms C(1), C(2), C(6), C(8), C(10), C(11), and Co(1) all lie on a mirror plane and the alternative C(3), C(5), C(7), and C(9) sites are produced by this mirror. With the nitrogen and sulfur sites, the complex is complete. There is also a second set of nitrogen and sulfur sites produced by the mirror, but the remainder of the cage is effectively the same. Thus, $S(2^i)$ is bonded to C(6), $N(1^i)$ is bonded to C(3), etc. The large thermal ellipsoids for C(4), C(6), and C(8) are a result of the averaging of the two close sites, neither of which lies on the mirror. As a result of this the bond lengths and angles involving these atoms are not meaningful although the nitrogen and sulfur bond lengths connected with Co are well-defined. Selected bond lengths and angles are presented in Tables 3 and 4.

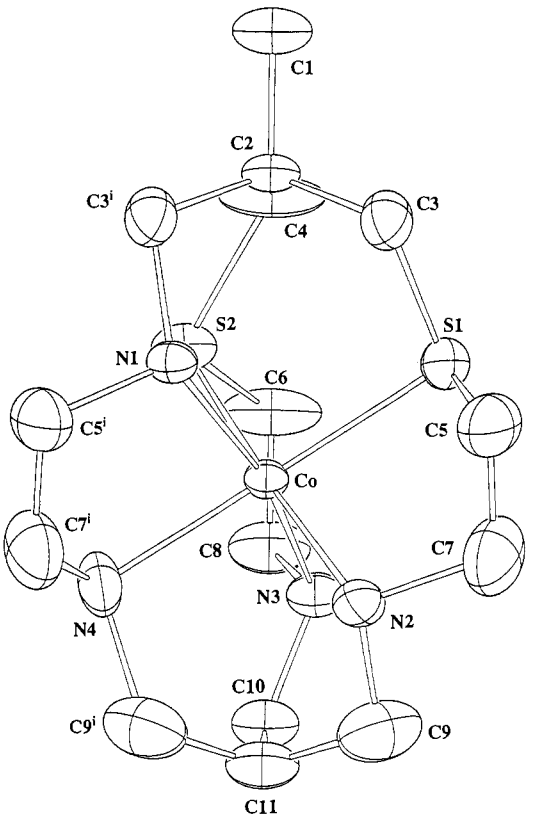

Figure 2. ORTEP[36] plot of the cation $[Co(HN_4S_2sar)]^{2+}$.

Table 3. Selected Bond Lengths (Å) for $[Co(HN_4S_2sar)](ClO_4)_2$

S(1)–Co(1)	2.288(2)	S(2)–Co(1)	2.495(2)
N(1)–Co(1)	2.104(6)	N(2)–Co(1)	2.151(7)
N(3)–Co(1)	2.039(7)	N(4)–Co(1)	2.114(7)

Table 4. Selected Bond Angles (deg) for $[Co(HN_4S_2sar)](ClO_4)_2$

S(2)–Co(1)–S(1)	91.8(1)	N(1)–Co(1)–S(1)	90.8(2)
N(1)–Co(1)–S(2)	87.1(2)	N(2)–Co(1)–S(1)	84.9(2)
N(2)–Co(1)–S(2)	171.9(2)	N(2)–Co(1)–N(1)	100.3(3)
N(3)–Co(1)–S(1)	126.9(2)	N(3)–Co(1)–S(2)	72.9(2)
N(3)–Co(1)–N(1)	136.7(3)	N(3)–Co(1)–N(2)	103.2(3)
N(4)–Co(1)–S(1)	169.1(3)	N(4)–Co(1)–S(2)	95.5(3)
N(4)–Co(1)–N(1)	81.6(3)	N(4)–Co(1)–N(2)	88.9(3)
N(4)–Co(1)–N(3)	63.2(3)		

The average Co–N bond length (2.102(7) Å) is shorter than that reported for the hexaaza complexes $[Co(diAZAN_6sar)]S_2O_6 \cdot H_2O$ (2.164 Å)[3] and $[Co(diAMN_6sarH_2)](NO_3)_4 \cdot H_2O$ (2.170 Å)[12] but is longer than that reported for the mixed-donor complex $[Co(AZAN_3S_3sar)](ClO_4)_2$ (2.076 Å).[27] A small elongation of the Co–N(2) bond *trans* to S(2) is observed. A marked elongation in the Co–S(2) bond (2.495(2) Å), in

Table 5. Redox Potentials of Complexes $[Co(XN_4S_2sar)]^{n+}$

complex	E^0,[a] mV (vs SHE)[c]	E^0,[b] mV (vs SHE)[c]
$[Co(N_4S_2)]^{3+/2+}$	−82	d
$[Co(NON_4S_2sar)]^{3+/2+}$	+22	+16
$[Co(AMN_4S_2sarH)]^{4+/3+}$	+22	+16
$[Co(CLN_4S_2sar)]^{3+/2+}$	−37	−41
$[Co(HN_4S_2sar)]^{3+/2+}$	−156	−158
$[Co(AZAN_4S_2sar)]^{3+/2}$	−84	−88

[a] 0.1 M $NaClO_4$. [b] 0.1 M $HClO_4$. [c] Pt auxiliary electrode, glassy carbon, T = 298 K, Ag/AgCl (saturated $NaClO_4$) reference electrode (+231 mV vs SHE) [d] Not measured.

comparison with the Co–S(1) bond (2.288(2) Å) is apparent. The short Co–S bond is similar to those observed in the structure of $[Co(Me_2S_6sar)](CF_3SO_3)_2$ (2.265(3), 2.279(3) Å)[23] which also displayed two significantly longer *trans* Co–S bonds (2.354(2) Å). Such elongation of the *trans* Co–S bonds has been observed in the structure of the complex $[Co([18])aneS_6)](picrate)_2$ (2.479(1) Å compared with $2.271(10)_{av}$Å) and ascribed to the low spin condition of the metal ion and the consequent Jahn–Teller distortion.[44,45] The conformation of the chelate rings in $[Co(HN_4S_2sar)]^{2+}$ is lel_3, since the C–C vectors of the five-membered chelate rings are parallel to the pseudo-C_3 axis of the complex, similar to the conformations observed in the Co(II) complexes $[Co(AZAN_3S_3sar)](ClO_4)_2$[27] and $[Co(Me_2S_6sar)](CF_3SO_3)_2$[23] and in contrast to the ob_2lel conformation seen for the Co(II) complex of the tripodal hexathia ligand 1,1,1-tris-(((2-(methylthio)ethyl)thio)methyl)ethane.[44]

The Co(II)–N bond length for $[Co(AZAN_3S_3sar)]^{2+}$ is significantly shorter (~0.1 Å) than that observed for the high-spin cobalt(II) hexaamine complexes,[2,27] and the solution magnetic moment of $[Co(AZAN_3S_3sar)]^{2+}$ indicates that this complex is low spin.[9,16] Although Jahn–Teller distortion, commonly associated with low-spin d^7 Co(II) ions, was not observed in the structure of $[Co(AZAN_3S_3sar)]^{2+}$,[27] the disorder problem associated with this complex cation resulted only in averaged values reported for Co(II)–S and Co(II)–N bond lengths.[27] The short average Co(II)–N bond length observed for the $[Co(AZAN_3S_3sar)]^{2+}$ ion has been attributed to the low-spin electronic state of the metal rather than resulting from strain-induced deformations.[27] It is apparent that the average Co(II)–N bond length for $[Co(HN_4S_2sar)]^{2+}$ is not characteristic of those found in either the high-spin N6 or the low-spin N3S3 complexes.

Magnetism. The solution magnetic moment for $[Co(AMN_4S_2sarH)]^{3+}$ (2.88 μ_B, 296 K) lies between values expected for low-spin or high-spin behavior in Co(II) complexes. The complex $[Co(AMN_3S_3sarH)]^{3+}$ exhibited a magnetic moment fully consistent with low-spin behavior under the same conditions (2.16 μ_B, 296 K). A variable-temperature study for the $[Co(AMN_4S_2sarH)]^{3+}$ complex in aqueous solution over a limited temperature range (293–333 K) resulted in a range for μ_{eff} of 2.85–3.08 μ_B. Under the same experimental conditions, the low-spin system $[Co(AZAN_3S_3sar)]^{2+}$ exhibited a range of μ_{eff} of 2.16–2.28 μ_B. From previous work it is apparent that the capping group of these macrocyclic ligands does not have a significant effect upon the spin state of the encapsulated Co(II) metal ion.[9]

Electrochemistry. The metal-based Co(III)/Co(II) reduction potentials for the range of $[Co(XN_4S_2sar)]^{n+}$ complexes, in both 0.1 M $NaClO_4$ and 0.1 M $HClO_4$, are listed in Table 5. $[Co(NON_4S_2sar)]^{3+/2+}$, $[Co(AMN_4S_2sarH)]^{4+/3+}$, $[Co(CLN_4S_2sar)]^{3+/2+}$, $[Co(AZAN_4S_2sar)]^{3+/2+}$, and $[Co(HN_4S_2sar)]^{3+/2+}$ exhibited quasi-reversible reduction waves with both gold and glassy carbon working electrodes and in both solvent systems. The $[Co(NON_4S_2sar)]^{3+/2+}$ system exhibited the expected irreversible reducitons characteristic of the NO_2 group.[8] At scan rates greater than 500 mV s^{-1} the cyclic voltammetric reduction waves generally exhibited increasingly irreversible characteristics.

Table 6. Bimolecular Rate Constants (k_{12})[a] for Outer-Sphere Electron Transfer Reactions and Calculated Self-Exchange Rate Constants (k_{11}) for $[Co(XN_4S_2sar)]^{n+/(n-1)+}$

reactants	k_{obs}, s^{-1}	k_{12}, M^{-1} s^{-1}	k_{11}[b] M^{-1} s^{-1}
$[Co(AMN_4S_2sarH)]^{4+}$ + $[Co(AMMEN_6sarH)]^{3+}$ [c]	1.77	0.76×10^3	$0.72(0.20) \times 10^3$
$[Co(CLN_4S_2sar)]^{3+}$ + $[Co(AMMEN_6sarH)]^{3+}$ [d]	0.79	3.35×10^2	$0.84(0.20) \times 10^3$
$[Co(CLN_4S_2sar)]^{3+}$ + $[Co(diCLN_6sar)]^{2+}$ [e]	2.00	1.07×10^3	$1.71(0.16) \times 10^3$
$[Co(HN_4S_2sar)]^{3+}$ + $[Co(AMMEN_6sarH)]^{3+}$ [f]	0.12	5.38×10^1	$1.84(0.30) \times 10^3$
$[Co(AZAN_4S_2sar)]^{3+}$ + $[Co(AMMEN_6sarH)]^{3+}$ [g]	0.32	1.39×10^2	$1.12(0.22) \times 10^3$

[a] Aqueous solution (0.1 M $HClO_4$/0.1 M $NaClO_4$), 298 K. [b] k_{11} calculated from the Marcus correlation. [c] [Co(III)] 1.35×10^{-4} M; [Co(II)] 2.31×10^{-3} M. [d] [Co(III)] 2.63×10^{-4} M; [Co(II)] 2.36×10^{-3} M. [e] [Co(III)] 1.87×10^{-3} M; [Co(II)] 2.03×10^{-4} M. [f] [Co(III)] 1.95×10^{-4} M; [Co(II)] 2.23×10^{-3} M. [g] [Co(III)] 2.86×10^{-4} M; [Co(II)] 2.32×10^{-3} M.

The magnitude of the N_4S_2sar couples conforms to the expectation that they would be intermediate between the reduction potentials exhibited by the analogous N_6sar and N_3S_3sar complexes. The Co(II) species is stabilized with increasing number of thioethers in the first coordination sphere of the metal ion, reflected by the more positive reduction potential in comparison with those of cobalt hexaamines.[8,23,46] The gradation of donor sets (N_6sar, N_4S_2sar, N_3S_3sar) produces a series of reductants or oxidants which retain their integrity upon reaction and for which the reduction potential can be finely tuned by variation in the capping group. The introduction of the thioether donors obviously enables access to a potential range not spanned by the cobalt N_6sar complexes.[8,15]

Electron Transfer Studies. The self-exchange rate constant for electron transfer for $[Co(AMMEN_6sar)]^{4+/3+}$ was determined by direct means.[47] The chiral form of one oxidation state was mixed with the catoptric form of the other (Δ-$[Co(AMMEN_6sarH)]^{4+}$ 6.863×10^{-3} M; Λ-$[Co(AMMEN_6sarH)]^{3+}$ 6.875×10^{-3} M) and the change in optical rotation measured as a function of time. The rate law for the self-exchange reaction was

$$-d[\ln(\alpha_t - \alpha_0)]/dt = k_{11}[Co]_{total} = k_{obsd}$$

k_{11}, the self exchange rate constant for $[Co(AMMEN_6sarH)]^{4+/3+}$ was found to be 0.15 M^{-1} s^{-1} (25 °C, 0.1 M $NaClO_4$/0.1 M $HClO_4$), very similar to the value previously calculated from the cross reaction of $[Co(AMMEN_6sarH)]^{4+}$ with Cr(II) (0.1 M^{-1} s^{-1}).[15]

The kinetics of the outer-sphere one-electron reduction of $[Co(XN_4S_2sar)]^{n+}$ by $[Co(AMMEN_6sarH)]^{3+}$ were measured by stopped flow methods under pseudo-first-order conditions:

$$[Co(AMMEN_6sarH)]^{3+} + [Co(XN_4S_2sar)]^{n+} \rightarrow [Co(AMMEN_6sarH)]^{4+} + [Co(XN_4S_2sar)]^{(n-1)+}$$

The oxygen-sensitive Co(II) complex $[Co(AMMEN_6sarH)]^{3+}$ was held in excess in the reactions. In addition, the reaction of $[Co(diCLN_6sar)]^{2+}$ with $[Co(CLN_4S_2sar)]^{3+}$ was studied.

Table 6 reports bimolecular rate constants (k_{12}) for reactions between the $[Co(XN_4S_2sar)]^{n+}$ complexes (X = AM, n = 4; X = CL, H, AZA, n = 3), i.e. cobalt(III), and $[Co(AMMEN_6sarH)]^{3+}$ or $[Co(diCLN_6sar)]^{2+}$, i.e. cobalt(II). The bimolecular rate constants for the cross reactions were obtained under pseudo-

(44) Thorne, C. M.; Rawle, S. C.; Admans, G. A.; Cooper, S. R. *J. Chem. Soc., Chem. Commun.* **1987**, 306.
(45) Hartman, J. R.; Hintsa, E. J.; Cooper, S. R. *J. Am. Chem. Soc.* **1986**, *108*, 1208.
(46) Gahan, L. R.; Lawrance, G. A.; Sargeson, A. M. *Inorg. Chem.* **1984**, *23*, 4369.
(47) Dwyer, F. P.; Sargeson, A. M. *J. Phys. Chem.* **1961**, *65*, 1892.

Table 7. Self Exchange Rates of Electron Transfer for Encapsulated Complexes (298 K)

complex	medium	k_{11}, M^{-1} s^{-1}	ref
$[Co(diAZAN_6sar)]^{3+/2+}$	0.2 M NaCl	5.1	2, 3
$[Co(AZAMEN_6sar)]^{3+/2+}$	0.2 M NaCl	2.1	15
$[Co(diAMN_6sar)]^{3+/2+}$	0.2 M $LiClO_4$, pH 7.5[a]	0.5	15
$[Co(diAMN_6sarH_2)]^{5+/4+}$	0.2 M $LiClO_4$/ 0.2 M $HClO_4$	0.024	15
$[Co(diCLN_6sar)]^{3+/2+}$	0.2 M NaCl	3.0	5
$[Co(CLMEN_6sar)]^{3+/2+}$	0.2 M NaCl	2.4	5
$[Co(diHN_6sar)]^{3+/2+}$	0.2 M NaCl	2.1	15
$[Co(AMMEN_6sar)]^{4+/3+}$	0.1 M $NaClO_4$/ 0.1 M $HClO_4$	0.15	*b*
$[Co(AZAN_3S_3sar)]^{3+/2+}$		2.2×10^4	23
$[Co(AMN_4S_2sarH)]^{4+/3+}$	0.1 M $NaClO_4$/ 0.1 M $HClO_4$	0.72×10^3	*b*
$[Co(Me_2S_6sar)]^{3+/2+}$		2.8×10^4	23

[a] *N*-Ethylmorpholine buffer. [b] This work.

first-order conditions, the rate law being of the form

$$\text{rate} = k_{12}[\text{Co(III)}][\text{Co(II)}]$$

The self-exchange electron transfer rates (k_{11}) for the $[Co(XN_4S_2sar)]^{n+}$ complexes were calculated by using the Marcus correlation[25,26]

$$k_{12} = (k_{11}k_{22}K_{12}f_{12})^{1/2}$$

where $\log f_{12} = (\log K_{12})^2/(4 \log(k_{11}k_{22})/Z^2)$. Here k_{12} is the cross reaction rate constant, k_{22} is the self exchange rate constant for $[Co(AMMEN_6sarH)]^{4+/3+}$ or $[Co(diCLN_6sar)]^{3+/2+}$, K_{12} is the equilibrium constant, and Z is the collision frequency (10^{11} M^{-1} s^{-1}). In this formulation the work terms are not considered. Rate constants (k_{11}) calculated using this correlation are shown in Table 6. It is apparent that the electron transfer rates for the $[Co(XN_4S_2sar)]^{n+/(n-1)+}$ complexes calculated from the Marcus cross correlation are on the order of 10^3 M^{-1} s^{-1} and that the electron transfer rates are faster than those reported for the $[Co(XN_6sar)]^{3+/2+}$ complexes[15] and of a similar order to those reported for $[Co(Me_2S_6sar)]^{3+/2+}$ and $[Co(AZAN_3S_3sar)]^{3+/2+}$ (Table 7).[16,23]

Weaver and Lee have observed large disagreements between measured rate constants and predicted values for reactions with very large thermodynamic driving forces.[48] These discrepancies were said to be due to large unfavorable work terms required to form the collision complex prior to electron transfer. The extended Marcus correlation[30]

$$k_{12} = (k_{11}k_{22}K_{12}f_{12})^{1/2}W_{12}$$

has been employed to investigate the contribution of these work terms. Here, $W_{12} = \exp[-(w_{12} + w_{21} - w_{11} - w_{22})/2RT]$. $w(r)$, the work terms, are described by the Debye–Hückel theory

$$w(r) = z_2z_3(\Delta e)^2/(4\pi\epsilon_0D_sr(1 + \beta r\mu^{1/2}))$$

where $\beta = (8\pi N(\Delta e)^2/(1000D_s(4\pi\epsilon_0)kT))^{1/2}$, μ is the ionic strength of the reactant solution, and D_s is the static dielectric constant of the medium.[30] The results of these calculations are reported in Table 8. It is evident that the work term, although greater for reactions involving highly charged species, makes at most a factor of 2 difference in the final rate. The result is in agreement with previous workers who have shown that for these complexes the work terms generally have an insiginificant effect on the calculated rate of exchange for the Co(III)/Co(II) couple.[15]

The direct determination of the self exchange rates for the $[Co(XN_4S_2sar)]^{n+}$ complexes was undertaken using NMR methods, as the results of the cross reactions indicated a reaction rate too fast to be measurable by the polarimetric method.

Table 8. Comparison of Measured Bimolecular Rates of Exchange with Those Generated from the Extended Marcus Equation (298 K)

reactants	$k_{12(obs)}$, M^{-1} s^{-1}	$k_{12(calc)}$[a] M^{-1} s^{-1}	$k_{12(calc)}$[b] M^{-1} s^{-1}	ref
$[Co(diAMN_6sarH_2)]^{5+}$ – $[Co(diAZAN_6sar)]^{2+}$	1.4×10^2	1.0×10^2	3.4×10^2	15
$[Co(AMN_4S_2sarH)]^{4+}$ – $[Co(AMMEN_6sarH)]^{3+}$	0.76×10^3	1.6×10^3	1.3×10^3	*c*
$[Co(HN_4S_2sar)]^{3+}$ – $[Co(AMMEN_6sarH)]^{3+}$	54	1.5×10^2	1.8×10^2	*c*

[a] k_{12} calculated from the Marcus equation using directly determined values of k_{11} and k_{22}. [b] k_{12} including work terms calculated from the extended Marcus equation with directly determined values of k_{11} and k_{22}. [c] This work.

A common approach to the determination of the electron transfer self-exchange rate probes the effect of added paramagnetic ions on the width of an NMR resonance of a diamagnetic species.[16,49–55] In this case, the reaction considered is between diamagnetic cobalt(III) and paramagnetic cobalt(II):

$$\text{Co(II)} + \text{Co(III)} \overset{k_{11}}{\rightleftharpoons} \text{Co(III)} + \text{Co(II)}$$

Although it is the electron that exchanges, it is though the Co(III) and Co(II) nuclei are effectively exchanging in solution. Mathematically this may be represented by

$$T_2^{-1} = T_{2A}^{-1} + \tau_A^{-1}$$

provided that the frequency difference between individual reactant species is greater than the rate of exchange.[41,49] In this expression T_2^{-1} is the observed transverse relaxation time for the mixture A + B (= $\pi\nu_{1/2}$, where $\nu_{1/2}$ is the line width of the site (A + B)), T_{2A}^{-1} the transverse relaxation time of species A and τ_A^{-1} is the lifetime in A (=k_{11}[A]). The expression simplifies to[49]

$$\nu_{1/2} = \nu^0_{D1/2} + k_{obs}[P]$$

where now $\nu^0_{D1/2}$ is the width at half-height of the diamagnetic species, $\nu_{1/2}$ is the width at half-height of the diamagnetic species as paramagnetic species is added, $k_{obs} = (k_{11}/\pi)$, k_{11} is the self-exchange rate constant, and [P] represents the concentration of the paramagnetic species. It is in this form that the majority of line-broadening experiments are reported. An internal reference is normally used to establish the extent of paramagnetic broadening, theoretically enabling correction of the observed line widths as the concentration of the paramagnetic species is increased. The encapsulated complexes examined in this work possess a methyl peak for which the ^1H NMR resonance is both intense and well separated from the remainder of the spectrum, and attempts were made to study the broadening of this resonance in the presence of added Co(II) complex. For these experiments the Co(III)/Co(II) mixtures were prepared in such a way that the diamagnetic species was always in constant excess. The concentrations of the Co(III) and Co(II) species, resulting in the greatest possible line broadening, were dictated by the solubility of the Co(II) species. Upon examination of the spectra obtained from the $[Co(AMN_4S_2sarH)]^{4+/3+}$ and $[Co(HN_4S_2sar)]^{3+/2+}$ exchanges, it was found that for the diamagnetic species only, the line width of the internal reference (dioxane) and of the CH_3

(48) Weaver, M. J.; Lee, E. L. *Inorg. Chem.* **1980**, *19*, 1936.
(49) Swift, T. J.; Connick, R. E. *J. Chem. Phys.* **1962**, *37*, 307.
(50) Doine, H.; Swaddle, T. W. *Can. J. Chem.* **1990**, *68*, 2228.
(51) Doine, H.; Swaddle, T. W. *Inorg. Chem.* **1990**, *30*, 1858.
(52) Chandrasekhar, S.; McAuley, A. *Inorg. Chem.* **1992**, *31*, 480.
(53) Bernhard, P.; Sargeson, A. M. *Inorg. Chem.* **1988**, *27*, 2582.
(54) Vande Linde, A. M. Q.; Juntunen, K. L.; Mols, O.; Ksebati, M. B.; Ochrymowycz, L. A.; Rorabacher, D. B. *Inorg. Chem.* **1991**, *30*, 5037.
(55) Smolenaers, P. J.; Beattie, J. K. *Inorg. Chem.* **1986**, *25*, 2259.

signal were not necessarily the minimum within a data set, as expected. Further, the line shape of the singlets, specifically the CH_2 from the dioxane and the CH_3, was often distorted; asymmetric singlets or multiplets were often observed for these resonances. Finally, the line width of the reference did not vary in a systematic way with increasing addition of paramagnetic complex. As a result of these observations it was found that the observed ^1H line width for the "zero" point was not the natural line width of the CH_3 signal but was in fact the sum of the natural line width and a component determined by field inhomogeneity. When line width is plotted against [Co(II)], the first point, corresponding to the diamagnetic line width, deviated significantly from the average correlation. Strictly speaking, this "zero" point is the only point which must lie on the resultant line from the line-broadening experiments. A consistent and linear relationship between the observed change in line width and the concentration of the paramagnetic substance was not obvious. The observation suggested that (i) neither the dioxane nor the encapsulated complex experiences paramagnetic broadening, although the dioxane may be more susceptible to field inhomogeneities since it reflects these variations more than the CH_3, or (ii) the dioxane may experience some paramagnetic broadening whereas the encapsulated complex does not. On the basis of the observations of this experiment, diamagnetic species in solution with a paramagnetic source are not necessarily broadened to the same extent. It appears, therefore that the general rule of adding an "innocent" reference is not the most reliable method of establishing the effect of a paramagnetic source upon a diamagnetic species. Although increasing the concentration of the paramagnetic Co(II) species would result in both a greater exchange-induced line broadening and decrease the effect of the random sources of broadening, the limited solubility of the Co(II) species and the necessity of pseudo-first-order conditions prohibited such a solution. An added deterrent to increasing reactant concentrations is the high ionic strength which would result from the 4+/3+ and 3+/2+ encapsulated complexes and the subsequent effect on the work terms. In the instance of the $[Co(AMN_4S_2sarH)]^{4+/3+}$ and $[Co(HN_4S_2sar)]^{3+/2+}$ systems with the line-broadening experiment it is the rate of exchange which is the restricting parameter overall, since systems possessing faster rates of self exchange (e.g. 10^6 M^{-1} s^{-1}) would exhibit proportionally greater line broadening for similar reactant concentrations, and therefore be less susceptible to the random errors discussed here.

The electron transfer reaction was subsequently investigated through determination of T_2. The requirement that the exchanging system is within the slow exchange region on the NMR time scale was established by determining whether the condition $(\omega_{Co(III)} - \omega_{Co(II)})^2 \gg T_2^{-2}, \tau^{-2}$ was met.[41,49] Here, $\omega_{Co(III)} - \omega_{Co(II)}$ is the chemical shift difference (in radians) between the exchanging sites. The resonance positions for the CH_3 in the cobalt(II) complexes were available from the NMR studies, and thus the frequency differences for the resonant positions of the CH_3 in the Co(III) and Co(II) complexes were determined as 2.08×10^4 rad s^{-1} for $[Co(AMN_4S_2sarH)]^{4+/3+}$ and 1.53×10^4 rad s^{-1} for $[Co(HN_4S_2sar)]^{3+/2+}$. From the Marcus correlations, estimations for the self-exchange rates of the $[Co(XN_4S_2sar)]^{3+/2+}$ complexes were available, and calculations indicated that the slow exchange conditions were met for these systems.

The intensity decay of the methyl ^1H NMR resonance for each encapsulated complex studied was monitored with delay time, τ, and the exponential

$$I/I_0 = \exp(-t/T_2) + c$$

where $t = 2\tau$, was fitted to the data. In this equation I_0 represents the initial intensity of the magnetisation, I the intensity after time t (i.e. after 2τ), and c the residual intensity of the magnetisation after $t = 4T_2$ (which should be approximately zero). The rate constant k_{11} was obtained after plotting $2/T_2$ (the time constant for the rate of decay of the exponential) against [Co(II)] (Figure 3). Half of the slope of this line is k_{11}. For the complexes $[Co(AMN_4S_2sarH)]^{4+/3+}$ and $[Co(HN_4S_2sar)]^{3+/2+}$ the electron transfer self-exchange rates (k_{11}) were determined to be 1.7(0.5) $\times 10^3$ $M^{-1}s^{-1}$ and 1.22(0.2) $\times 10^4$ $M^{-1}s^{-1}$, respectively. Within the limitations of the Marcus theory,[15,25,26] there is good agreement between the self-exchange rates determined by direct and indirect methods. However, the small driving force for the reaction involving $[Co(HN_4S_2sar)]^{3+}$ and $[Co(AMMEN_6sar)]^{3+}$ places a limit on the usefulness of the calculated self-exchange rate for the former complex.

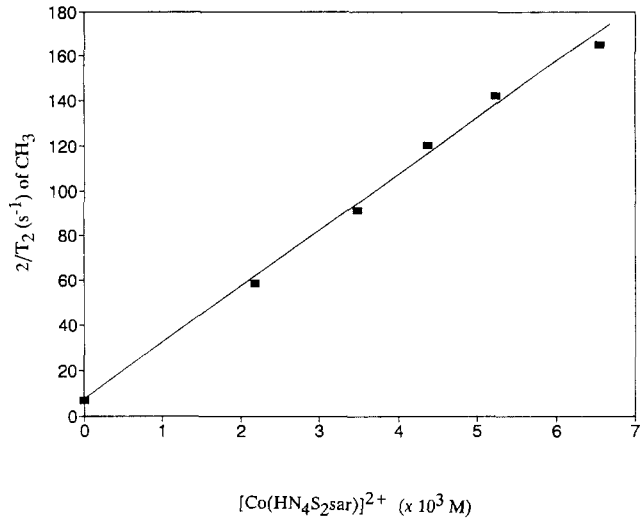

Figure 3. Plot of $2/T_2$ vs $\{[(Co(HN_4S_2sar)]^{2+}\}$ for the determination of the self-exchange rate of $[Co(HN_4S_2sar)]^{2+}$.

The self-exchange rate constants for the series of encapsulated complexes $[Co(XN_{6-x}S_xsar)]^{n+/(n-1)+}$ (x = 6, 3, 2, 0) presented in Table 7 span 6 orders of magnitude. While the accelerating influence of thioether donors on electron transfer for cobalt(III)/cobalt(II) complexes has been noted previously,[16,56] the presence of more thioether donors does not necessarily imply a larger self-exchange rate constant. For example, there is little difference between the rate constants reported for the $[Co(AZAN_3S_3sar)]^{3+/2+}$ and $[Co(Me_2S_6sar)]^{3+/2+}$ complexes (2.4×10^4 M^{-1} s^{-1} and 2.8×10^4 M^{-1} s^{-1}, respectively).[23] There does, however, appear to be a progressive increase in the self exchange rate constant through the series $[Co(XN_{6-x}S_xsar)]^{(n-1)+/n+}$ (x = 0, 2, 3), a series also related by the progressive change in the nature of the spin-state changes associated with the Co(II)/Co(III) electron transfer process (high spin/low spin, intermediate spin/low spin, low spin/low spin).

Simplistically these spin-state changes, and any associated bond length changes, may be employed to calculate inner-sphere reorganization energies (ΔG_{in}^*) for the process. The inner-shell reorganization energy is given by

$$\Delta G_{in}^* = {}^1/_2\{f_{III}f_{II}/(f_{III} + f_{II})\}[\Delta d]^2$$

where f_{III} and f_{II} are the bond stretching force constants, and $[\Delta d]$ is the difference in the equilibrium bond distance, in the two oxidation states.[30,57,58] The application of this expression has some limitations. The expression is misleading as it assumes that symmetrical breathing modes convey the reaction;[59] however, complicated coupling between Co–N and internal ligand motions and conformational equilibria may contribute to the reorganiza-

(56) Küppers, H.-J.; Neves, A.; Pomp, C.; Ventur, D.; Wieghardt, K.; Nuber, B.; Weiss, J. *Inorg. Chem.* **1986**, *25*, 2400.
(57) Marcus, R. A.; Sutin, N. *Biochim. Biophys. Acta* **1985**, *811*, 265.
(58) Endicott, J. F.; Brubaker, G. R.; Ramasami, T.; Kumar, K.; Dwarakanath, K.; Cassel, J.; Johnson, D. *Inorg. Chem.* **1983**, *22*, 3754.
(59) Stanbury, D. M.; Lednicky, L. A. *J. Am. Chem. Soc.* **1984**, *106*, 2847.

tion.[58] A further limitation in the determination of ΔG_{in}^* lies with the magnitude of the symmetrical force constants employed in the calculation. Force constants reported for Co(III)–N lie in the range 147–186 N m^{-1},[60-66] although values as high as 245 and 248 N m^{-1} have been reported.[57,58] Similarly, for Co(II)–N values of 80–82 N m^{-1} are commonly employed,[60,61,64] although values as high as 128–139 N m^{-1} have been reported.[58,67] In this work we use 248 N m^{-1} (Co(III)) and 139 N m^{-1} (Co(II)).[58,67] For the Co(III)–S and Co(II)–S force constants a value of 110 N m^{-1} is commonly used in the former case,[66] and 70–90 N m^{-1} for the latter.[27] We have also assumed that the Co–S and Co–N bond lengths for $[Co(AMN_4S_2sarH)]^{4+}$ and $[Co(HN_4S_2sar)]^{3+}$ would not be significantly different from those in $[Co(NON_4S_2sar)]^{3+}$;[11] similarly, the Co(II)–N/S distances for $[Co(AMN_4S_2sarH)]^{3+}$ are not significantly different from those observed in $[Co(HN_4S_2sar)]^{2+}$.

As a result of the limitations outlined above, the calculation of ΔG_{in}^* is subject to some uncertainty (±25%);[58] however, the general trends are informative. The complexes $[Co(AZAN_3S_3sar)]^{2+}$ (Δd = 0.07 (N), 0.09 (S) Å) and $[Co(Me_2S_6sar)]^{2+}$ (Δd = 0.06 Å) are low-spin systems[16,23] and the calculated inner-sphere reorganization energies are 7 and 3 kJ mol^{-1}, respectively. The result suggest that the similarities in self-exchange rate for $[Co(AZAN_3S_3sar)]^{2+}$ and $[Co(Me_2S_6sar)]^{2+}$ arise from similar internal reorganization energies, which are related to the low-spin condition of the Co(II).[23,27] For the high-spin system $[Co(diAZAN_6sar)]^{2+}$ the internal reorganization barrier is larger (ΔG_{in}^* = 49 kJ mol^{-1}; Δd = 0.17 Å).[2,15] For $[Co(AMN_4S_2sarH)]^{4+/3+}$ and $[Co(HN_4S_2sar)]^{3+/2+}$, ΔG_{in}^* (18 kJ mol^{-1}; Δd = 0.09 (N), 0.18 (S) Å) falls between the average limits observed for low-spin/high-spin and low-spin/low-spin electron transfer, consistent with the magnitude of the magnetic susceptibility, intermediate between high and low spin, displayed by this complex.

The relationship between redox reactivity and the inner-sphere reorganization energy of a series of metal complexes has been explored previously using the Marcus–Sutin model for electron transfer.[28-31,56] In this model the inner-sphere modes are treated in a quantum mechanical way, where the emphasis upon achieving a specific configuration prior to electron transfer is lifted. The electron transfer is thought of in terms of an ion-pair preequilibrium, the exchange rate constant expressed as the product of a preequilibrium constant, K_0, the effective nuclear frequency, ν_n, and nuclear, κ_n, and electronic factors, k_{el}.[31]

$$k = K_0 \nu_n \kappa_n \kappa_{el}$$

The preequilibrium constant K_0, the effective nuclear frequency, ν_n, and the nuclear, κ_n, and electronic factor, κ_{el}, have been defined previously.[31] It is generally assumed that the exchange reactions are adiabatic and that κ_{el} = 1. ΔG_{out}^* and Γ_λ have their usual meanings.[31] We have applied this model for the complexes $[Co(AZAN_3S_3sar)]^{3+/2+}$, $[Co(Me_2S_6sar)]^{3+/2+}$, $[Co(AMN_4S_2sarH)]^{4+/3+}$, $[Co(HN_4S_2sar)]^{3+/2+}$, and $[Co(diAZAN_6sar)]^{3+/2+}$. The results of the calculations are reported in Table 9 and suggest that for all of the complexes the preequilibrium constants (K_0), the work terms (w_r), and the outer-sphere reorganization energies (ΔG_{out}^*) remain essentially constant, although the work terms for the $[Co(AMN_4S_2sarH)]^{4+/3+}$ complex reflect the greater charge present. The self-exchange rates calculated from this semiclassical approach may be compared with experimentally determined values (Table 9). It is seen that there is very little difference between the values for the hexaamine systems. However, as the number of sulfur donors in the coordination sphere of the metal ion increases and the electron transfer occurs between low-spin/low-spin states rather than low-spin/high-spin states, variations of an order of magnitude or greater between the measured self-exchange rate and the predicted values are obvious. Such variations have been observed previously for other systems.[56,68] The expression for the self exchange rate constant in the Marcus–Sutin model may be expanded[31] to the form

$$-[\ln(k_{11}/(K_0\nu_n\Gamma_\lambda)) + \Delta G_{out}^*/RT] = \Delta G_{in}^*/RT - \ln \kappa_{el}$$

The relationship encompasses differing force constants and nuclear and electronic factors and implicitly considers the magnitude of the difference in bond lengths between the oxidized and reduced forms of the complexes. A plot of $-[\ln(k_{11}/(K_0\nu_n\Gamma_\lambda)) + \Delta G_{out}^*/RT]$ versus $\Delta G_{in}^*/RT$ should be linear, and theoretically the slope of the line should be 1.0 with a zero intercept predicted for κ_{el} = 1.0.[31] When this analysis is applied to the encapsulated complexes considered in this work (and for $[Co(en)_3]^{3+/2+}$,

Table 9. Comparison of Directly Determined Self-Exchange Rate Constants for Selected $[Co(XN_{6-x}S_xsar)]^{n+}$ Complexes (x = 0, 2, 3, 6) with Rate Constants for Electron Exchange Calculated from Semiclassical Theories (I = 0.2 M)

	1	2	3	4	5
r,[b] Å	9.0	9.0	9.0	9.0	9.0
Δd, Å	0.17[b,c]	0.09 (N) 0.18 (S)	0.09 (N) 0.18 (S)	0.07 (N)[d] 0.09 (S)	0.06[e]
w_r, kJ mol^{-1}	5.0	5.0	10.0	5.0	5.0
K_0, M^{-1}	6×10^{-2}	6×10^{-2}	1×10^{-2}	6×10^{-2}	6×10^{-2}
ΔG_{out}^*, kJ mol^{-1}	21	21	21	21	21
ΔG_{in}^*, kJ mol^{-1}	49	18	18	7	3
Γ_λ	5	1	1	1	1
k_{11},[f] M^{-1} s^{-1}	1.8	6.6×10^4	8.6×10^3	3.9×10^6	1.2×10^7
k_{11},[g] M^{-1} s^{-1}	5.1[c]	1.3×10^4 [h]	1.7×10^3 [h]	2.4×10^4 [i]	2.8×10^4 [i]

[a] Key: $[Co(diAZAN_6sar)]^{3+/2+}$ (**1**); $[Co(HN_4S_2sar)]^{3+/2+}$ (**2**); $[Co(AMN_4S_2sarH)]^{4+/3+}$ (**3**); $[Co(AZAN_3S_3sar)]^{3+/2+}$ (**4**); $[Co(Me_2S_6sar)]^{3+/2+}$ (**5**). [b] Reference 31. [c] References 2 and 15. [d] Reference 27. [e] The Co(III) Co-S bond lengths range between 2.230 and 2.235 Å.[23] [f] k_{11} calculated from the semiclassical Marcus–Sutin theory. [g] k_{11} determined by direct means. [h] Average of the k_{11} results obtained from T_2 experiments. [i] Reference 23.

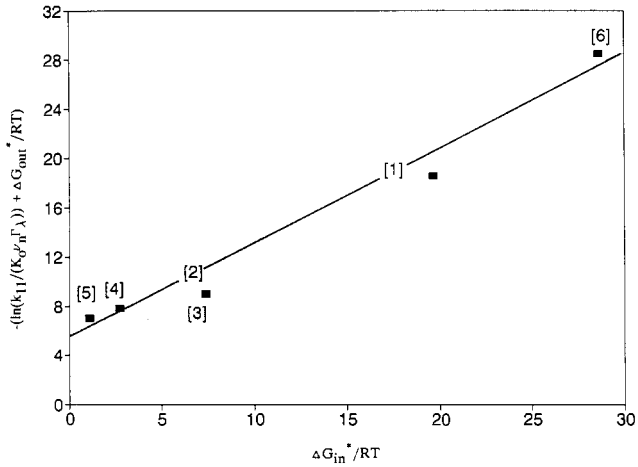

Figure 4. Plot of $\Delta G_{in}^*/RT$ vs $-(\ln(k_{11}/K_0\nu_n\Gamma_\lambda) + \Delta G_{out}^*/RT)$. Key: (1) $[Co(diAZAN_6sar)]^{3+/2+}$; (2) $[Co(HN_4S_2sar)]^{3+/2+}$; (3) $[Co(AMN_4S_2sarH)]^{4+/3+}$; (4) $[Co(AZAN_3S_3sar)]^{3+/2+}$; (5) $[Co(Me_2S_6sar)]^{3+/2+}$; (6) $[Co(en)_3]^{3+/2+}$ (data taken from ref 31).

(60) Nakagawa, I.; Shimanouchi, T. *Spectrochim. Acta* **1966**, *22*, 759.
(61) Schmidt, K. H.; Müller, A. *Inorg. Chem.* **1975**, *14*, 2183.
(62) DeHayes, L. J.; Busch, D. H. *Inorg. Chem.* **1973**, *12*, 1505.
(63) Hambley, T. W.; Hawkins, C. J.; Palmer, J. A.; Snow, M. R. *Aust. J. Chem.* **1981**, *34*, 45.
(64) Williamson, B. E.; Dubicki, L.; Harnung, S. E. *Inorg. Chem.* **1988**, *27*, 3484.
(65) Stynes, H. C.; Ibers, J. A. *Inorg. Chem.* **1971**, *10*, 2304.
(66) Laier, T.; Larsen, E. *Acta Chem. Scand.* **1979**, *A33*, 257.
(67) Siders, P.; Marcus, R. A. *J. Am. Chem. Soc.* **1981**, *103*, 741.
(68) Brown, G. M.; Sutin, N. *J. Am. Chem. Soc.* **1979**, *101*, 883.

considered as a precursor to the hexaamine encapsulated complexes), a linear correlation between k_{11} and ΔG_{in}^{*} is suggested (slope 0.8) (Figure 4) although a positive intercept is apparent. The result obtained is similar to that reported for other series of chromium(III)/chromium(II), ruthenium(III)/ruthenium(II), iron(III)/iron(II), and cobalt(III)/cobalt(II) complexes encompassing amine,[31] oxygen,[31] and thioether ligands[56] and implies that the overall analysis is too simplistic.[31]

Acknowledgment. We thank Professor Alan Sargeson and the Research School of Chemistry, The Australian National University, Australia, for access to the Perkin-Elmer P22 spectropolarimeter and the Gibbs Durrum D-110 stopped flow equipment.

Supplementary Material Available: Listings of full crystal data (Table S1), thermal parameters (Table S2), hydrogen atom positional and thermal parameters (Table S3), bond distances and bond angles (Table S4), torsion angles (Table S5), and experimental kinetic data (Tables S6–S10) (11 pages). Ordering information is given on any current masthead page.